How to cite: *Angew. Chem. Int. Ed.* **2021**, *60*, 7654–7658
International Edition: doi.org/10.1002/anie.202017001
German Edition: doi.org/10.1002/ange.202017001

Supramolecular Chemistry

Photo-Controllable Catalysis and Chiral Monosaccharide Recognition Induced by Cyclodextrin Derivatives

*Lei Chen, Yong Chen, Yi Zhang, and Yu Liu**

Dedicated to the 100th anniversary of Chemistry at Nankai University

Abstract: *A supramolecular catalytic system was constructed from polycationic α-cyclodextrin (**6-Iz-α-CD**) and gold nanoparticles (**AuNP**) using a supramolecular assembly strategy. The cavity of cyclodextrin is the channel by which the substrate molecules come into contact with the catalytic center. Introduction of the azobenzene-modified diphenylalanine (**Azo-FF**) guest molecule allowed for precise photo-control of the catalytic activity owing to its sensitive response to irradiation. Importantly, as a unique glucose oxidase the **AuNP@6-Iz-α-CD** realizes unprecedented chiral recognition catalysis for chiral monosaccharides. In combination with a 3,3′,5,5′-tetramethylbenzidine (TMB) color reaction, **AuNP@6-Iz-α-CD** is able to recognize the chirality of various monosaccharides.*

Intelligent supramolecular assemblies are a hot topic of research owing to their potential applications for nanomedicine,[1] nanomaterials,[2] catalysis,[3] and chiral molecular recognition.[4] Considerable effort has been devoted to preparing intelligent supramolecular materials that respond to external stimuli such as enzymes,[5] pH,[6] and light.[7] Among these stimuli, light is unique in that it can be delivered instantaneously to the responsive unit without hindrance by steric constraints or solvent viscosity.[8] Many light-responsive compounds have been reported.[9] Azobenzene derivatives are considered to be ideal triggers because their affinity for the cavities of cyclodextrins changes markedly upon irradiation, a property that has prompted research on the use of light to regulate the functional properties of supramolecular assemblies.[10] For instance, we recently reported paclitaxel-modified β-cyclodextrin and arylazopyrazole assemblies that can be used for photo-control of microtubule aggregation in cells via a specific interaction between paclitaxel and microtubules and reversible binding between the arylazopyrazoles and β-cyclodextrin.[11]

Gold nanoparticles (**AuNP**) are widely recognized as promising building blocks for intelligent supramolecular assemblies because their optical and catalytic properties depend on their aggregation state.[3b,12] One way to dynamically regulate their aggregation state is to use host–guest interactions. The usual method for accomplishing such regulation is to covalently attach host molecules directly to the **AuNP** surface and then add an appropriate guest molecule that acts as a cross-linking agent to promote **AuNP** aggregation.[13] However, light-controlled regulation of the aggregation state and catalytic activity of **AuNP** in supramolecular systems remains relatively unexplored. In addition, the use of **AuNP** for selective catalysis has not been explored. Almost all host molecules have the ability to distinguish substrates, such as chiral cavities in cyclodextrins for enantiomers recognition. Thus, to develop **AuNP** for selective catalysis, we undertook to incorporate them into supramolecular assemblies held together by non-covalent interactions. Herein, we report the development of catalytic supramolecular assemblies held together by electrostatic interactions between **AuNP** and the polycationic cyclodextrin hexakis-(6-iodo-6-deoxy)-α-cyclodextrin (**6-Iz-α-CD**).[14] An optically responsive azobenzene-modified diphenylalanine (**Azo-FF**) guest molecule was used to regulate the catalytic activity of the **AuNP@6-Iz-α-CD** through triggering a reversible morphological transition upon irradiation (Scheme 1). Importantly, the recognition of chiral molecules by **6-Iz-α-CD** cavity can realize the selective catalytic oxidation of glucose with different configurations.[15] Based on the chiral recognition catalysis oxidation ability of the **AuNP@6-Iz-α-CD** for chiral monosaccharide, combined with the color reaction of 3,3′,5,5′-tetramethylbenzidine (TMB), provides an unprecedented conveniently way for colorimetric recognition of chiral monosaccharide.

The **AuNP** were prepared by a sodium citrate reduction method,[15] and their particle size was verified by transmission electron microscopy (TEM) (average size = 17 nm; Supporting Information, Figure S1a). The surface of the **AuNP** is covered with citrate groups and the potential of **AuNP** is −64 mV (Figure S1b) and the **6-Iz-α-CD** host molecules were synthesized by previously reported method (Supporting Information, Scheme S1, Figure S2),[16] To verify that mixing the **AuNP** and **6-Iz-α-CD** resulted in coverage of the **AuNP** by **6-Iz-α-CD**, we performed UV-vis spectroscopy and zeta potential measurements. In **AuNP** aqueous solution, the increase of **6-Iz-α-CD** concentration results in surface potential changes from negative potential to positive potential and accompanied by the blue shift and then red shift of the surface plasmon resonance (SPR) absorption band (Figure 1 a,b) which indicated the **AuNP** experienced the process of dispersion in aqueous solution, aggregation and redispersion (Figure S3).[17] By monitoring the change of the absorption value of nanoparticles at 525 nm, it is determined that the

[*] L. Chen, Dr. Y. Chen, Y. Zhang, Prof. Dr. Y. Liu
College of Chemistry, State Key Laboratory of Elemento-Organic Chemistry, Nankai University
Tianjin 300071 (P. R. China)
E-mail: yuliu@nankai.edu.cn

Supporting information and the ORCID identification number(s) for the author(s) of this article can be found under: https://doi.org/10.1002/anie.202017001.

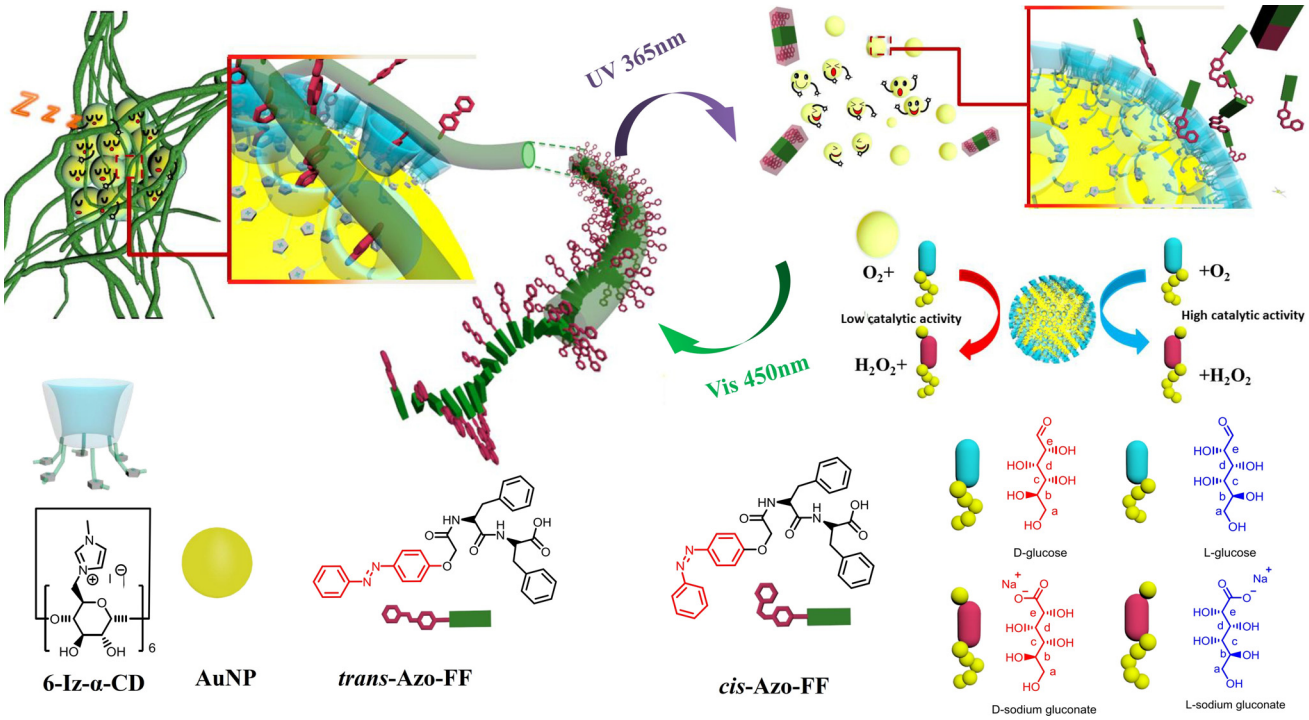

Scheme 1. Photo-control of the catalytic activity of **AuNP@6-Iz-α-CD** assemblies and chiral recognition catalytic process.

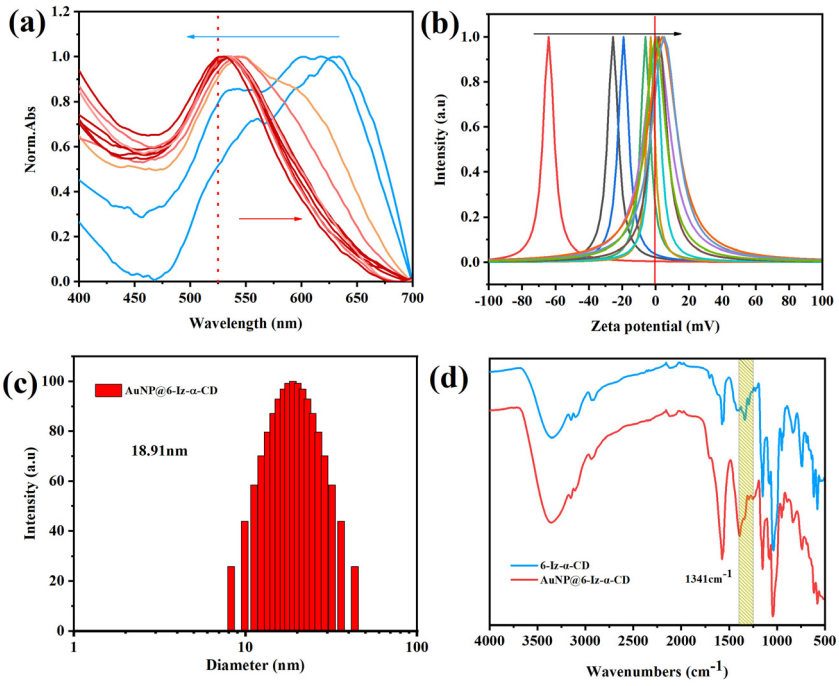

Figure 1. a) SPR of **AuNP** after addition of **6-Iz-α-CD** at various concentrations. b) Zeta potentials of **AuNP** at various **6-Iz-α-CD** concentrations ([Au] = 7.96×10^{-4} g L^{-1}, [**6-Iz-α-CD**] = 0 M–1.8×10^{-4} M). c) DLS analysis of **AuNP@6-Iz-α-CD** in aqueous solution. d) Fourier-transform IR spectra of **6-Iz-α-CD** and **AuNP@6-Iz-α-CD**.

uniform dispersion of **AuNP@6-Iz-α-CD** can be formed when the concentration of **AuNP** is 7.96×10^{-4} g L^{-1} and the concentration of **6-Iz-α-CD** is 4×10^{-5} M (Figure S3a). The dynamic light scattering (DLS) test confirmed that the particle size of the assembly is in accordance with the theoretical value (theoretical value 18.57 nm, Figure 1c; Scheme S2). Moreover, Fourier transform IR spectroscopy show that the peak for the stretching vibration of the methylimidazole moiety of **6-Iz-α-CD** (1341 cm^{-1}) is clearly weaker in the spectrum of **AuNP@6-Iz-α-CD**, which confirms the presence of electrostatic interactions between **6-Iz-α-CD** and the **AuNP** (Figure 1d). In order to further confirm the number of **6-Iz-α-CD** on the **AuNP** surface, the thermogravimetric analysis was carried out on the **AuNP@6-Iz-α-CD**. It can be calculated that there are 2606 **6-Iz-α-CD** per **AuNP** by thermogravimetry data and formula calculation (Figure S4).

The reduction of 4-nitrophenol (4-NP) with sodium borohydride ($NaBH_4$) at 25 °C was used as a model reaction to evaluate the catalytic activity of **AuNP@6-Iz-α-CD** and the reaction process was monitored by UV-vis spectroscopy.[18] Firstly, **AuNP** exhibit high catalytic activity and the reaction is pseudo first order with respect to the absorbance (Figure 2a; Figure S5, $K_{app} = 3.97\times10^{-3}$ s^{-1}). Surprisingly, the catalytic process of **AuNP@6-Iz-α-CD** seems to be different from the above kinetic reaction process (Figure 2b). Hence, the circular dichroism spectroscopy was used to monitor the catalytic reaction process of **AuNP@6-Iz-α-CD**, it was found that the reaction process of 4-NP was

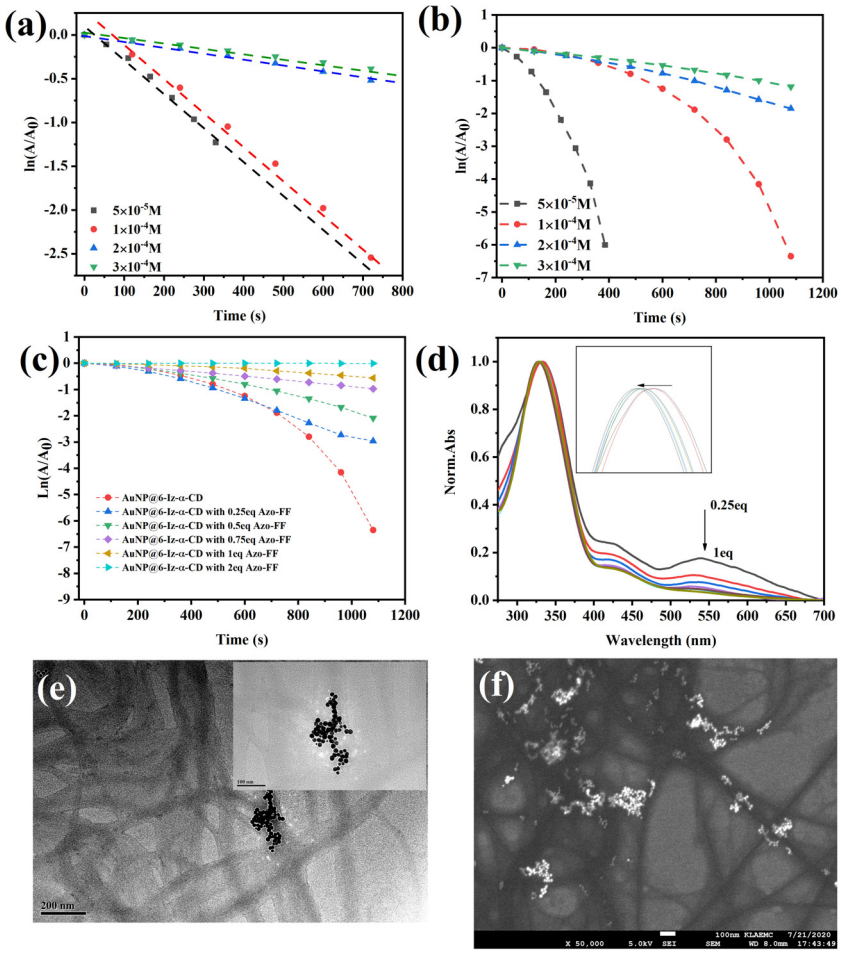

Figure 2. The reduction of 4-NP catalyzed by a) **AuNP** b) **AuNP@6-Iz-α-CD** ([Au] = 7.96×10^{-4} g L^{-1}, [**6-Iz-α-CD**] = 4×10^{-5} M, [4-NP] = 5×10^{-5}–3×10^{-4} M) c) **AuNP@6-Iz-α-CD** + **Azo-FF** ([**Azo-FF**] = 0–8×10^{-5} M, [4-NP] = 1×10^{-4} M). d) Changes of UV absorption of **AuNP@6-Iz-α-CD** with different equivalents of **Azo-FF.** e) The morphology of the **AuNP@6-Iz-α-CD** + **Azo-FF** observed by TEM and f) SEM.

carried out in the cavity of α-cyclodextrin (Figure S6). The catalytic reaction of the substrate in the cyclodextrin cavity has aroused our attempts to control the activity of the catalyst. Hence, using previously described methods,[10b] we synthesized azobenzene guest molecules **Azo-FF**, for controlling the activity of the catalytic assemblies (Figures S7–S9). Indeed, with the increase concentration of **Azo-FF** in the catalytic system, the 4-NP reduction model verified that the catalytic activity of the assembly decreased significantly (Figure 2c; Figures S10 and S11). However, the addition of at least two equivalents **Azo-FF** is required to make the catalytic system dormant. Therefore, the assemble model between **Azo-FF** and **AuNP@6-Iz-α-CD** were study in detail. As shown in Figure 2d, the blue shift of UV absorption peak at 325 nm of azobenzene group and strong circular dichroism signal indicate that azobenzene group enters into the cyclodextrin cavity through host–guest interaction (Figure S12).[19] Interestingly, the SPR absorption band belonging to **AuNP** gradually disappeared with the addition of **Azo-FF**, which indicated the formation of the assembly is accompanied by the detachment of **AuNP** from the solvent system. Combined with TEM and scanning electron microscopy (SEM), it was found that **AuNP** are surrounded by fibers (Figure 2e,f; Figure S13a–c), and **AuNP** accumulated along with the extension direction of the fiber. Based on the above results, it is speculated that the process of catalytic activity dormancy of supramolecular assembly is as follows: with the additional of **Azo-FF**, the incorporation of azobenzene into the cyclodextrin cavity does hinder the binding of the substrate molecules to the catalytic site through the cyclodextrin cavity, However, host–guest interaction is a dynamic equilibrium process, which could not completely block the substrate molecules from entering the cyclodextrin cavity. Therefore, the diphenylalanine (L-Phe-L-Phe, FF) peptide part of **Azo-FF** is needed to promote the aggregation of **AuNP@6-Iz-α-CD** through the π-π stacking among aromatic units. Furthermore, excessive **Azo-FF** tend to self-assemble to form one-dimensional oriented fiber structure and then form a large-scale fiber network structure (Figure S14a,b), which separate the **AuNP@6-Iz-α-CD** from the solution system and lead the catalytic activity of the assembly dormant. As expected, when **AuNP@6-Iz-α-CD** + **Azo-FF** is exposed to UV irradiation, the network formed by *trans*-**Azo-FF** dissociates and *trans*-**Azo-FF** is converted to *cis*-**Azo-FF** (Figure S14c,d), whereupon it exits the α-cyclodextrin cavity, releasing the **AuNP@6-Iz-α-CD** and awakening their catalytic activity (Figure S13d–f). Moreover, because **Azo-FF** responds rapidly to irradiation, the catalytic activity of the **AuNP@6-Iz-α-CD** + **Azo-FF** system can be dynamically regulated by alternating irradiation with UV and visible light (Figures S15 and S16).

Many research groups have reported that **AuNP** can act as an artificial enzyme to catalyze the conversion of glucose to gluconic acid and hydrogen peroxide (H_2O_2).[20] Inspired by these reports, **AuNP@6-Iz-α-CD** was also tested as a glucose oxidase. The catalytic oxidation of glucose was monitored by TMB chromogenic assay (Figures S17 and S18). Interestingly, **AuNP@6-Iz-α-CD** exhibits obvious recognition catalysis performance at high substrate concentration, and the difference of chiral monosaccharide catalysis become more obvious with the increase of time (Figure 3a–d). The catalytic oxidation of D-glucose (D-Glu) by **AuNP@6-Iz-α-CD** seems to be blocked, and the products of catalytic oxidation do not increase with time but the catalytic process of L-glucose (L-Glu) is not affected. We speculate that the difference in catalytic selectivity for different chiral glucose is due to the recognition of chiral substances in the cavity of **6-Iz-α-CD**.

To confirm this hypothesis, D-sodium gluconate was added into the **AuNP** and **AuNP@6-Iz-α-CD** respectively. It is found that D-sodium gluconate only inhibits the catalytic activity of the **AuNP@6-Iz-α-CD** (Figure S19). On the other hand, α-cyclodextrin was directly modified on nanoparticles (**AuNP + α-CD**) as a control group (Figures S20 and S21).[21] However, there is no significant difference in the catalytic oxidation of different chiral glucose. Hence, we inferr the following mechanism for chiral recognition and catalysis by the **AuNP@6-Iz-α-CD** (Figure 3e,f). The aldehyde group of D- or L-Glu contact with the **AuNP** through the cyclodextrin and undergoes **AuNP**-catalyzed oxidation to the corresponding sodium gluconate. However, the α-cyclodextrin cavity of **6-Iz-α-CD** has a stronger affinity for D-Glu than for the corresponding enantiomers[22] (Figures S22–S25) and the imidazole group modified α-cyclodextrin makes the surface of **AuNP** positively charged. Hence, the higher bonding of the **6-Iz-α-CD** cavity to the oxidation products of D-configuration glucose and the attraction of the positive charge on the surface of the assembly prevent the separation from the α-cyclodextrins cavity (Figure S26). Finally, the process of D-glucose catalyzed by supramolecular catalyst is terminated. However, the affinity between sodium L-gluconate and cyclodextrin cavity is negligible (Figure S27), so there is no effective host–guest interaction between them. L-Glu can squeeze it out of the cavity and continue the catalytic process. Based on the above characteristics, combined with the color reaction process of TMB, the chirality of monosaccharide can be easily and quickly judged by naked eyes. We subjected three pentoses (lyxose, ribose, and xylose) and a hexose (mannose) to the same catalytic process. For all the monosaccharide, the **AuNP@6-Iz-α-CD** can effectively distinguish enantiomers (Figure 4).

In summary, we constructed supramolecular assemblies comprising **6-Iz-α-CD** and **AuNP. AuNP@6-Iz-α-CD** assemblies acted as a catalytic center. Intriguingly, the introduction of **Azo-FF** endowed the supramolecular assembly with the ability of precise optical regulation of catalytic activity. Furthermore, **AuNP@6-Iz-α-CD** demonstrated unprecedented special glucose oxidase activity and was able to distinguish between the enantiomers of monosaccharide substrates. These characteristics of **AuNP@6-Iz-α-CD** were utilized in the rapid colorimetric recognition of different chiral monosaccharides, which could quickly and effectively recognize the chirality of monosaccharides. Herein, we provide a convenient way to prepare a supramolecular catalyst with an intelligent response; moreover, the new application of the cyclodextrin cavity is found by combining the supramolecular assembly concept with catalysis. The findings provide a foundation for the development of supramolecular assemblies in the field of catalysis.

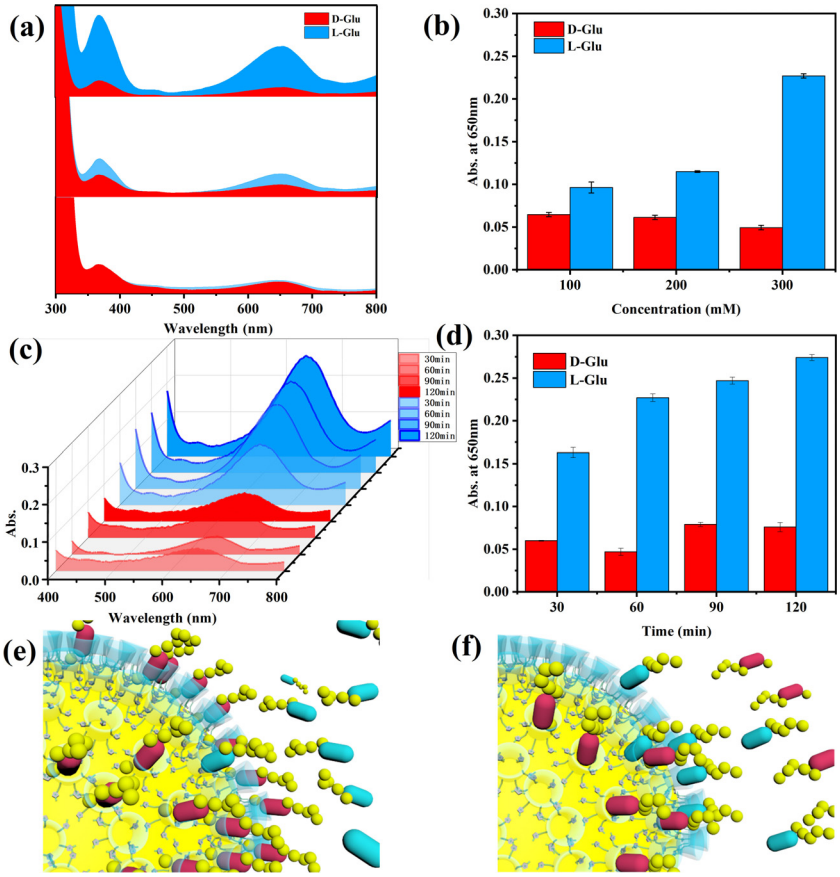

Figure 3. a,b) Catalysis mediated by **AuNP@6-Iz-α-CD** at different concentrations and with different chiral substrates. c,d) Catalysis mediated by **AuNP@6-Iz-α-CD** over varying durations and with different chiral substrates. e,f) Simulation of the catalytic process of assembly for different chiral monosaccharides.

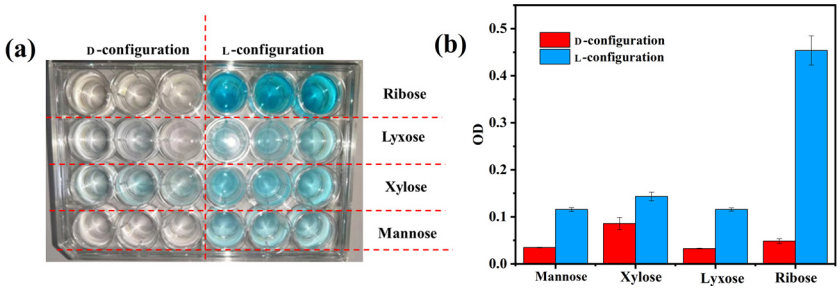

Figure 4. Rapid color recognition of different chiral monosaccharide by **AuNP@6-Iz-α-CD**.

Acknowledgements

We thank NNSFC (21861132001, 21971127, 21772099) for financial support.

Conflict of interest

The authors declare no conflict of interest.

Keywords: catalysis · chirality recognition · cyclodextrins · photo-controllable · supramolecular assembly

[1] Z. Xu, S. Jia, W. Wang, Z. Yuan, B. J. Ravoo, D.-S. Guo, *Nat. Chem.* **2019**, *11*, 86 – 93.
[2] H.-L. Sun, Y. Chen, X. Han, Y. Liu, *Angew. Chem. Int. Ed.* **2017**, *56*, 7062 – 7065; *Angew. Chem.* **2017**, *129*, 7168 – 7171.
[3] a) Q. Zhang, D.-H. Qu, Q.-C. Wang, H. Tian, *Angew. Chem. Int. Ed.* **2015**, *54*, 15789 – 15793; *Angew. Chem.* **2015**, *127*, 16015 – 16019; b) Q. Zhang, W.-Z. Wang, J.-J. Yu, D.-H. Qu, H. Tian, *Adv. Mater.* **2017**, *29*, 160494.
[4] a) J. Huang, P. Su, B. Zhao, Y. Yang, *Anal. Methods* **2015**, *7*, 2754 – 2761; b) X. Yao, H. Zheng, Y. Zhang, X. Ma, Y. Xiao, Y. Wang, *Anal. Chem.* **2016**, *88*, 4955 – 4964.
[5] a) D.-S. Guo, T.-X. Zhang, Y.-X. Wang, Y. Liu, *Chem. Commun.* **2013**, *49*, 6779 – 6781; b) V. U. Rein, *J. Mater. Chem.* **2006**, *16*, 2217 – 2225.
[6] J. Nanda, A. Biswasa, A. Banerjee, *Soft Matter* **2013**, *9*, 4198 – 4208.
[7] a) L. Chen, Y. Chen, H.-G. Fu, Y. Liu, *Adv. Sci.* **2020**, *7*, 2000803; b) S. Yagai, A. Kitamura, *Chem. Soc. Rev.* **2008**, *37*, 1520 – 1529.
[8] Y.-H. Wei, S.-B. Han, J. Kim, S. Soh, B. A. Grzybowski, *J. Am. Chem. Soc.* **2010**, *132*, 11018 – 11020.
[9] a) J. Guo, H.-Y. Zhang, Y. Zhou, Y. Liu, *Chem. Commun.* **2017**, *53*, 6089 – 6092; b) G. Liu, Y.-M. Zhang, L. Zhang, C. Wang, Y. Liu, *ACS Appl. Mater. Interfaces* **2018**, *10*, 12135 – 12140; c) R. Klajn, *Chem. Soc. Rev.* **2014**, *43*, 148 – 184.
[10] a) Y. Takashima, S. Hatanaka, M. Otsubo, M. Nakahata, T. Kakuta, A. Hashidzume, *Nat. Commun.* **2012**, *3*, 1270; b) W. Zhang, Y. Chen, J. Yu, X.-J. Zhang, Y. Liu, *Chem. Commun.* **2016**, *52*, 14274 – 14277.
[11] Y.-M. Zhang, N.-Y. Zhang, K. Xiao, Q. Yu, Y. Liu, *Angew. Chem. Int. Ed.* **2018**, *57*, 8649 – 8653; *Angew. Chem.* **2018**, *130*, 8785 – 8789.
[12] W. Rechberger, A. Hohenau, A. Leitner, J. R. Krenn, B. Lamprecht, F. R. Aussenegg, *Opt. Commun.* **2003**, *220*, 137 – 141.
[13] H. Li, D.-X. Chen, Y.-L. Sun, Y. B. Zheng, L.-L. Tan, P. S. Weiss, *J. Am. Chem. Soc.* **2013**, *135*, 1570 – 1576.
[14] J.-J. Li, Y. Chen, J. Yu, N. Cheng, Y. Liu, *Adv. Mater.* **2017**, *29*, 1701905.
[15] a) H. Wei, E. Wang, *Chem. Soc. Rev.* **2013**, *42*, 6060 – 6093; b) W.-J. Luo, C.-F. Zhu, S. Su, D. Li, Y. He, Q. Huang, C.-H. Fan, *ACS Nano* **2010**, *4*, 7451 – 7458.
[16] P. Hu, Y. Chen, Y. Liu, *Chem. Commun.* **2015**, *51*, 10839 – 10842.
[17] K. I. Assaf, A. Hennig, S. Peng, D.-S. Guo, D. Gabel, W. M. Nau, *Chem. Commun.* **2017**, *53*, 4616 – 4619.
[18] Y. Chen, Z. Wang, Y. W. Harn, S. Pan, Z. Li, S. Lin, *Angew. Chem. Int. Ed.* **2019**, *58*, 11910 – 11917; *Angew. Chem.* **2019**, *131*, 12036 – 12043.
[19] H. Yamaguchi, Y. Kobayashi, R. Kobayashi, Y. Takashima, A. Hashidzume, H. Akira, *Nat. Commun.* **2012**, *3*, 603.
[20] L. Gao, J. Zhuang, L. Nie, *Nat. Nanotechnol.* **2007**, *2*, 577 – 583.
[21] T. Huang, F. Meng, L. M. Qi, *J. Phys. Chem. C* **2009**, *31*, 13636 – 13642.
[22] W. Hirsch, T. Muller, R. Pizer, P. J. Ricatto, *Can. J. Chem.* **1995**, *73*, 12 – 15.

Manuscript received: December 22, 2020
Revised manuscript received: January 3, 2021
Accepted manuscript online: January 5, 2021
Version of record online: February 24, 2021

